Inorganic Chemistry
Article
Cite This: Inorg. Chem. XXXX, XXX, XXX−XXX
pubs.acs.org/IC

A Self-Doped Oxygen-Free High-Critical-Temperature (High-T_c) Superconductor: SmFFeAs

Dan Lin,[†] Han-Shu Xu,[‡] Jingjing Luo,[‡] Haoliang Huang,[§] Yalin Lu,[‡,§] and Kaibin Tang*[,†,‡]

[†]Department of Chemistry, University of Science and Technology of China, Hefei 230026, People's Republic of China

[‡]Hefei National Laboratory for Physical Sciences at Microscale, University of Science and Technology of China, Hefei 230026, People's Republic of China

[§]Anhui Laboratory of Advanced Photon Science and Technology, National Synchrotron Radiation Laboratory, University of Science and Technology of China, Hefei 230026, People's Republic of China

Supporting Information

ABSTRACT: A new iron-base superconductor SmFFeAs is synthesized via solid-state metathesis reaction by using SmFCl and LiFeAs as precursors. The compound crystallized in the tetragonal ZrCuSiAs-type structure with the space group *P*4/*nmm* and lattice parameters of a = 3.9399(0) Å and c = 8.5034(1) Å. The superconducting diamagnetic transition occurs at 56 K for the parent compound, which confirmed by the resistivity and magnetic susceptibility. The appearance of superconductivity without extrinsic doping could be ascribed to the self-doping owing to the mixed valence of Sm ions. The as-synthesized SmFFeAs serves as a new self-doped parent compound for oxygen-free high-critical-temperature (high-T_c) superconductors.

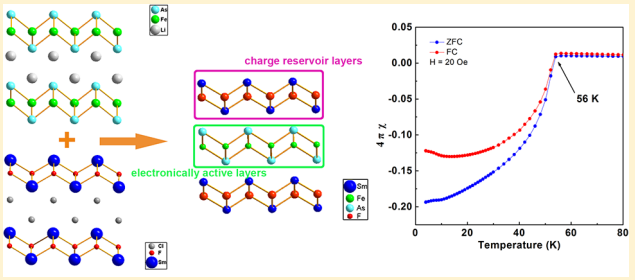

INTRODUCTION

Since the discovery of iron-arsenide superconductors (FeSCs), enormous impetus has been provided in the field of high-critical-temperature (high-T_c) superconductivity. In 2008, Kamihara et al. reported superconducting transition in the lanthanum-arsenide compound LaOFeAs (1111-type) by F-doping.[1] It was found that T_c changed with F content, exhibiting a maximum T_c = 26 K at a F^- content of 11 at. %. Subsequently, the T_c rapidly increases to above the theoretical value (39 K) predicted by McMillan[2] in the $LnFeAsO_{1-x}F_x$ (Ln = rare-earth elements) family. With the partly F-doping in the $SmFeAsO_{1-x}F_x$(x = 0.15), Chen et al. first reported that the new iron-based superconductors with the onset T_c of 43 K was obtained at ambient pressure.[3] After that, Zhao et al. discovered bulk superconductivity with the onset T_c value of >50 K in the $LnFeAsO_{1-x}F_x$ family[4−6] by a high-pressure (HP) synthesis method with replacing the La by other light rare-earth elements, such as Pr, Nd, Sm, etc. And, instead of chemical doping, Zhao et al. also succeeded in synthesizing the $LnFeAsO_{1-\delta}$ superconductors[7,8] with better superconductivity. Although these undoped iron arsenide (LnOFeAs) compounds do not exhibit superconductivity, previous works have shown that doping of electrons or holes can effectively induce superconductivity in this system. It is worth mentioning that all the aforementioned compounds are built up by almost identical Fe_2As_2 layers serving as a carrier conduction path, which are sandwiched between the insulating Ln_2O_2 layers. Moreover, experimental observations and theoretical studies suggest that the increase in T_c can be realized as a result of charge carriers doping in the two-dimensional electronic structure through ion substitution in the surrounding insulating layers.[9] Very recently, the quaternary fluoroarsenide AeFeAsF (Ae = Sr, Ca, etc.) has also been intensively studied as candidates for further exploration of high-T_c superconductors.[10−14] Through partial element substitution, the anomaly in resistivity, which is ascribed to the formation of a SDW order or a structural transition, was suppressed, which is similar to that observed in LnOFeAs and MFe_2As_2 systems.[15−17]

According to the above-mentioned studies, much effort has been done to understand the role of the modulation of the interactions to the superconductivity which occurs in iron-based systems upon suitable chemical doping of certain elements at the O or AE sites. Partial doping is likely the mostly common approach to obtain high-T_c superconductors. However, the doping process is always performed by using classic solid-state reactions, which require harsh experimental conditions including high temperature and high pressure, as well as long reaction time. It is still very difficult to obtain the pure target phase, because of the multiple raw materials. Besides, as indicated in the systems of LnOFeAs and AeFeAsF, superconductivity can indeed be introduced by doping, but overdoping would lead to the increase of impurities and the collapse of the structure,[13,18] which will lead to the absence of superconductivity. Therefore, it is worth exploring new

Received: August 16, 2019

DOI: 10.1021/acs.inorgchem.9b02464
Inorg. Chem. XXXX, XXX, XXX−XXX

compounds with high T_c by modifying the composition and reaction method in the future work.

Indeed, there are a few parent iron-based materials that exhibit superconductivity without extrinsic doping. The typical compounds are (i) AFe_2As_2(A = Na, K, Rb and Cs) (122),[19−22] (ii) $AeAFe_4As_4$ (Ae = Ca, Sr, Eu; A = K, Rb, Cs) (1144),[23−25] (iii) $ACa_2Fe_4As_4F_2$ (A = K, Rb, Cs) (12442),[26,27] (iv) Sr_2VO_3FeAs (21311),[28] (v) $Ba_2Ti_2Fe_2As_4O$ (22241),[29] and (vi) LnOFeP (Ln = La, Sm, Nd, Pr)[30,31] and ThNFeAs (1111),[32] which have been studied intensively. However, among the 1111-type iron-based compounds, only these two types of hosts without extrinsic doping LnOFeP and ThFeAsN exhibit superconducting properties. And previously reported studies[13,14] on AeFeAsF were limited to the cases of Ae being a divalent alkaline-earth element, while systems with divalent rare-earth elements have not been studied further. These results give us inspiration that further work is needed to complete the system of self-doped 1111-type FeSCs and investigate the mechanism of superconductivity.

Here, we report the synthesis of the new iron arsenide fluoride SmFFeAs with tetragonal ZrCuSiAs-type structure, which was obtained by totally substituting Sm_2F_2 layers for Sm_2O_2 layers through the solid-state metathesis (SSM) method,[33] instead of partial-doping method in the previous work. Importantly, the as-prepared sample SmFFeAs exhibits a T_c of 56 K without deliberate doping. Following with the LnOFeP and ThNFeAs, it can be inferred that the SmFFeAs sample presents as a new self-doped 1111-type superconductor that makes great contribution to the research of high-T_c iron-based superconductor.

EXPERIMENTAL SECTION

Synthesis. FeAs was synthesized by heating stoichiometric mixtures of high-purity Fe powder (Aladdin, 99.95%) and As powder (Aladdin, 99.95%) in sealed silica tube and then combined with stoichiometric amounts of Li (Aladdin, 99.9%) to synthesize LiFeAs by heating at 1073 K for 24 h. SmFCl was synthesized by heating the mixture of Sm (Aladdin, 99.9%), $SmCl_3$ (Aladdin, 99.9%), and SmF_3 (Aladdin, 99.99%) in a molar ratio of 1:1:1 at 873 K for 72 h in sealed alumina. The synthesis of SmFFeAs was performed by heating the mixture of LiFeAs and SmFCl in the molar ratio of 1:1, using the SSM method. All of the precursors were well-homogenized, placed in alumina crucibles, and then sealed in the silica tubes. The reaction mixtures were heated to 1073 K and maintained at that temperature for 48 h, followed by cooling to room temperature naturally. The co-formed byproduct LiCl was removed from the sample by evaporating at the reaction temperature. We applied annealing techniques in order to obtain higher-quality samples. The as-synthesized sample was treated at 773 K for 10 h in an evacuated quartz tube. All the sample preparations were performed in the argon-filled glovebox to protect the samples from oxygen.

Characterizations. The crystal structure of the sample was characterized with a Philips X'pert X-ray diffractometer (Cu Kα radiation, = 1.54182 Å) in the 2θ range of 10°−90° at room temperature. The XRD data was analyzed by the Rietveld fitting method using the GSAS suite. The morphology and structural characterization were examined via scanning electron microscopy (SEM) (Model S-4800), transmission electron microscopy (TEM) (Model Talos F200X), and selected-area electron diffraction (SAED) (Model Talos F200X). The surface chemical state was determined by X-ray photoelectron spectroscopy (XPS) (Thermo ESCALAB 250Xi), using Al Kα radiation. Magnetization measurements were performed with a vibrating sample magnetometry (VSM) system (Quantum Design), operated in the magnetic field of 20 Oe and in the temperature range of 4−200 K. The resistance data was collected by using DC four-probe technique on the Physical Property Measurement System (PPMS) (Quantum Design).

RESULTS AND DISCUSSION

Figure 1 shows the XRD pattern and its Rietveld refinement profile for the SmFFeAs sample. Table 1 lists the refined

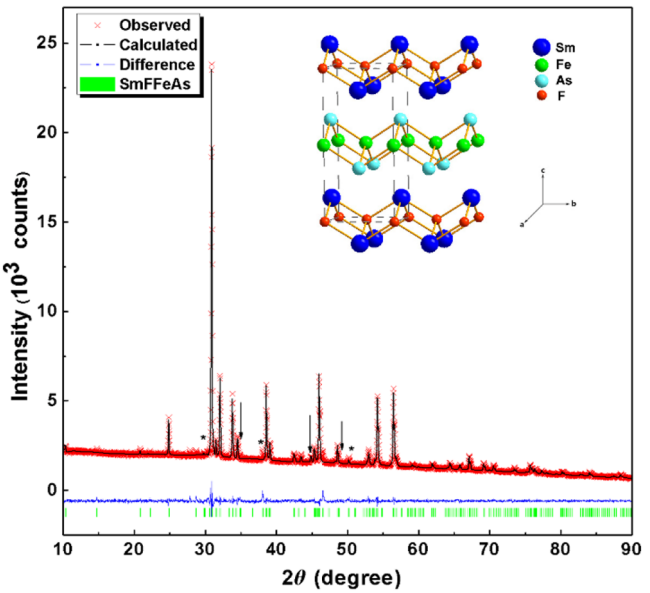

Figure 1. Rietveld refinement profile of the powder X-ray diffraction (XRD) of SmFFeAs. Arrows indicate peaks due to impurity phase FeAs. Asterisks indicate peaks due to impurity phase Fe_2As. The inset shows the crystal structure of SmFFeAs.

Table 1. Crystallographic Data of SmFFeAs at 300 K

parameter						
compound						SmFFeAs
space group						*P*4/*nmm*
a (Å)						3.9399(0)
c (Å)						8.5034(1)
c/*a*						2.1583
V (Å^3)						131.998 (5)
R_{wp} (%)						4.07
R_p (%)						3.20
χ^2						1.913
As−Fe−As angle (degree) × 2						110.208(1)
As−Fe−As angle (degree) × 4						109.104(0)
h_{As}[a] (Å)						1.374
atom	Wyckoff	occupancy	*x*	*y*	*z*	U_{iso}
Sm	2*c*	1.000	0.25	0.25	0.13781	0.0663
Fe	2*b*	1.000	0.75	0.25	0.5	0.0678
As	2*c*	1.000	0.25	0.25	0.66159	0.0680
F	2*a*	1.000	0.75	0.25	0	0.1248

[a] h_{As} represents the pnictogen height from the iron plane.

structural parameters. The crystal structure, phase purity, and lattice constants of the as-prepared sample powders were determined with the assistance of Rietveld refinement, using the 1111-type structure model and the program GSAS. The resultant reliability factor (R_p) is 0.0320, R_{wp} = 0.0407, and χ^2 = 1.913, which proves the correctness and validity of the refinement result. The main diffraction peaks of SmFFeAs can

DOI: 10.1021/acs.inorgchem.9b02464
Inorg. Chem. XXXX, XXX, XXX−XXX

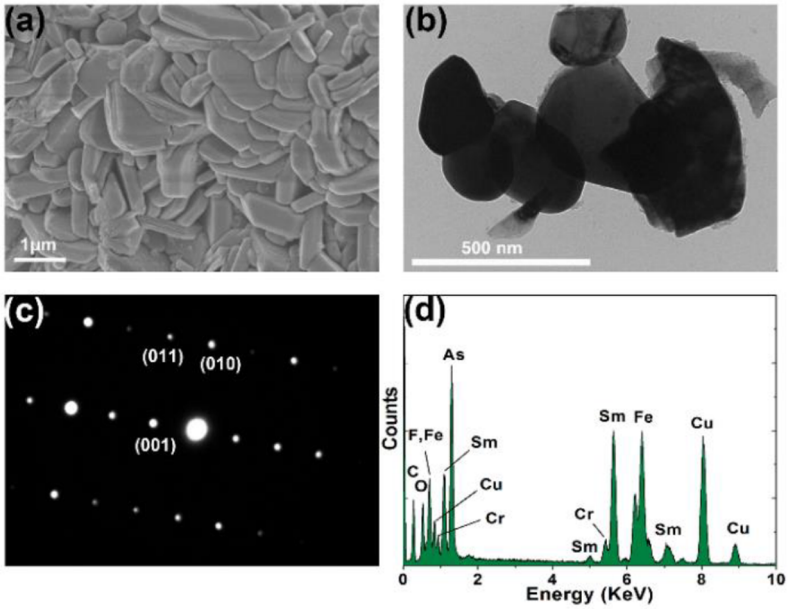

Figure 2. (a) SEM image, (b) TEM image, (c) SAED pattern, and (d) EDS spectrum of as-obtained SmFFeAs.

be well-indexed by the tetragonal structure with a = 3.9399(0) Å and c = 8.5034(1) Å. Only a small amount of impurity phases FeAs and Fe_2As are detected, which do not exhibit superconductivity during the measuring temperature range and will not cause interference in this study.[34,35] It is noted that the SmFFeAs crystal is also composed of two functional sheets alternately stacked along its c-axis direction, as shown in the inset of Figure 1. The iron arsenide $(FeAs)^-$ layers as the electronically active planes are sandwiched by samarium fluoride $(SmF)^+$ layers as the charge reservoir layers. Generally, the change of ionic radius in crystal structure will lead to the variation of cell parameters.[32] Comparing the lattice parameters between SmFFeAs and SrFFeAs, these two compounds only differ in the ion species at the AE site of AEFFeAs compounds and the ionic radius of Sm^{2+} (1.10 Å) is almost close to the value of Sr^{2+} (1.06 Å). The a-axis and c-axis of SmFFeAs are, respectively, 0.059 and 0.469 Å smaller than the counterparts of SrFFeAs[13]. The c-axis is decreased much more (by 5.23%) than the a-axis (by 1.48%).

It could be summarized that the c-axis has a tendency to be affected more significantly with the ion substitution at the AE site, which has also been the similar case in the previous work.[32] Moreover, compared with the SrFFeAs, the contraction of c-axis indicates that the interlayer bonding is strengthened, stabilizing the compound.[29]

In addition, the axial ratio c/a is also considered as an important parameter to characterize the crystalline lattice. We compare the c/a value of sample SmFFeAs with the $[Ln_2O_2]$-based 1111-type iron arsenides (data points coincide at $c/a \approx 2.16$) and $[AE_2F_2]$-based 1111-type iron arsenides ($c/a \approx 2.24$),[32] respectively. Cao et al. proposed, on the basis of many data, that the c/a values are closely related to the size of the ionic radii of Z^{n-} (Z^{n-} = F^-, O^{2-}). Here, we note that, although the ionic radii Z^{n-} of SmFFeAs is same with the AeFeAsF, the axial ratio $c/a \approx 2.158$ is similar to the value of LnOFeAs.

The morphology and structural features were characterized by SEM, TEM, and SAED. As illustrated in Figure 2a, SmFFeAs exhibits a typical platelike layered structure. Layered structures such as this provide the possibility and advantage of intercalation. The size of the grains ranges from 1 μm to 3 μm. Figure 2b shows a TEM image of SmFFeAs. The SAED pattern of SmFFeAs in Figure 2c reveals a single-crystal feature, which can be assigned to a tetragonal cell with $a = b$ = 3.9399(0) Å and c = 8.5034(1) Å. The diffraction spots are indexed to (010), (011), and (001) crystal planes matching well with the results of XRD pattern. Furthermore, the energy-dispersive X-ray spectroscopy (EDS) is employed to investigate the chemical composition of the as-obtained SmFFeAs. As shown in Figure 2d, elemental Sm, Fe, As, and F can be detected in the sample. The elemental O could be ascribed to the adsorbed oxygen on the sample surface, while the elemental Cu, C, and Cr would be ascribed to the sample grid and specimen room.

The XPS spectra was evaluated to further confirm the chemical states of the elements in the as-obtained SmFFeAs. The high-resolution Sm 3d spectrum of the as-obtained SmFFeAs is shown in Figure 3a. The two peaks with binding energy (BE) values of 1071.8 and 1109.4 eV correspond to Sm^{2+} $3d_{5/2}$ and $3d_{3/2}$ for SmFFeAs, respectively.[36] On the other hand, the peaks at 1082.6 and 1110.2 eV can be associated with Sm^{3+} $3d_{5/2}$ and $3d_{3/2}$.[36] The relative concentration of Sm^{3+} and Sm^{2+} was determined by calculating area of split peaks from the Figure 3a. We noted that the Sm^{3+} and Sm^{2+} states are 69.95% and 30.05%, respectively. It could speculate the coexistence of two valence states of Sm ions. Besides, it is known that the bond valence sum (BVS) has been used to determine the oxidation state of metal ions in solids.[37] The bond length could be analyzed by the BVS formula $S = \exp[(R_0 - R)/0.37]$, where each bond with a distance R contributes to the value S with R_0 as an empirical parameter. The total Sm-BVS calculated based on our measurement data is 2.112 in good agreement with the expected Sm valency. In Figure 3b, the two main peaks at 711.4 and 724.5 eV can be referred to Fe^{2+} $2p_{3/2}$ and $2p_{1/2}$ for SmFFeAs, respectively, while 714.2 and 727.5 eV could be attributed to Fe^{3+} in the impurity of FeAs and/or the sensitivity of sample to the air during the transfer.[38] Moreover, the peaks at 718.6 and 732.2

DOI: 10.1021/acs.inorgchem.9b02464
Inorg. Chem. XXXX, XXX, XXX−XXX

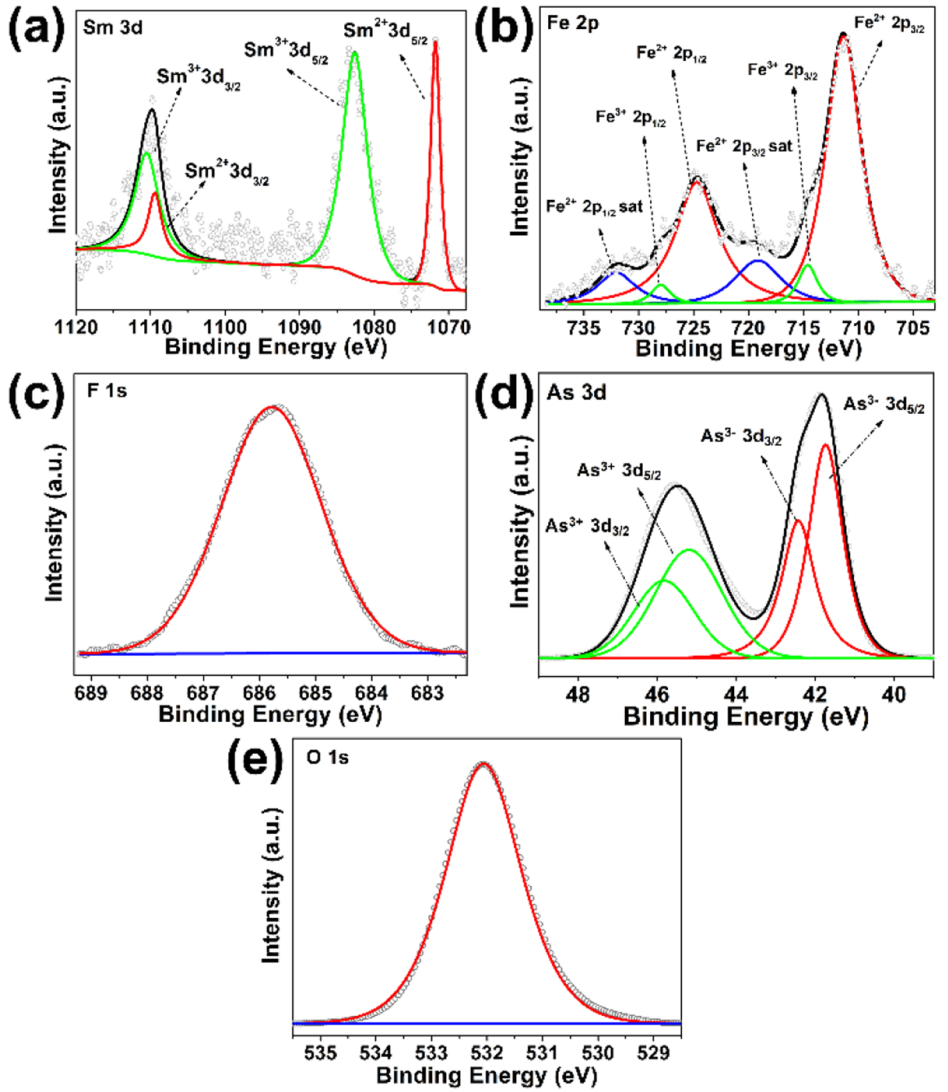

Figure 3. XPS spectra for the (a) Sm 3d, (b) Fe 2p, (c) F 1s, (d) As 3d, and (e) O 1s of the as-obtained sample SmFFeAs.

eV are ascribed to the satellite peaks of Fe^{2+} 2p.[39] As shown in Figure 3c, the peaks at 684.8 eV is assigned to F 1s of the Sm−F bond.[40] The peaks located at 41.1 and 41.7 eV are referred to As^{3-} $3d_{5/2}$ and $3d_{3/2}$ (in Figure 3d), respectively. The couple peaks at 45.2/45.8 eV could be associated with the oxidation states of arsenic, based on earlier study.[41] Figure 3e shows the binding energy of elemental O is 532.23 eV, corresponding to the adsorbed oxygen during the testing process or hydroxides with water contamination.[42,43] Compared with the doped compounds SmFeAs(O, F) (as shown in Figure S1 in the Supporting Information), it can be clearly seen that there are no splits in the peak of elemental O, which demonstrates that the as-obtained SmFFeAs is oxygen-free.

The temperature dependence of the magnetic susceptibility for the SmFFeAs is illustrated in Figure 4. Obvious diamagnetic signals are observed in both the field cooling (FC) and zero field cooling (ZFC) curves. The sharp superconducting transition at 56 K is quite higher than T_c = 30 K for ThFeAsN[32] and T_c = 4 K for LaOFeP.[30] Note that the upturn at <12 K could be ascribed to the small amount of other magnetic impurities in the sample. The upturn behavior is not caused by impurities FeAs and Fe_2As, because these two

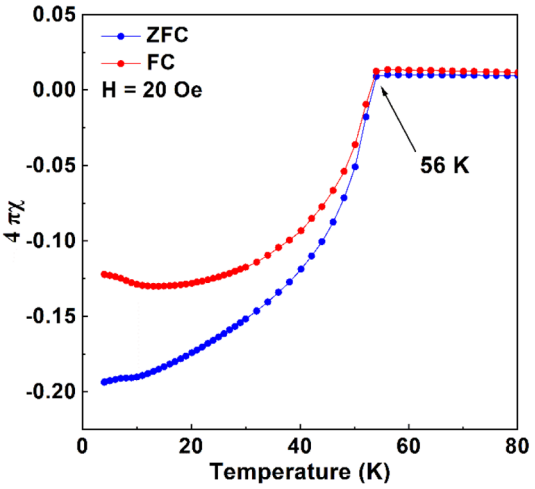

Figure 4. Temperature dependence of magnetic susceptibility for the as-synthesized sample, which is shown for zero-field cooled (ZFC) and field-cooled (FC) measurements at 20 Oe.

DOI: 10.1021/acs.inorgchem.9b02464
Inorg. Chem. XXXX, XXX, XXX−XXX

Table 2. Comparison of the Transition Temperature (T_c) among the As-Synthesized SmFFeAs in this Work and Other Representative High-T_c Iron-Based Compounds

compound[a]	space group	a (Å)	c (Å)	As−Fe−As α (deg)	As−Fe−As β (deg)	T_c (K)	ref
$(Gd_{0.8}Th_{0.2})OFeAs^{[HP]}$	$P4/nmm$	3.916	8.438	113.82	107.34	56	48
$Sm(O_{0.9}F_{0.1})FeAs^{[HP]}$	$P4/nmm$	3.915	8.428	112.63	107.91	55	5
$Sm(O_{0.85}F_{0.15})FeAs^{[AP]}$	$P4/nmm$	3.932	8.490	112.48	107.99	43	3
$Li_x(NH_3)_yFe_2Se_2^{[HP]}$	$I4/mmm$	3.770	16.973	100.61	114.07	55	49
$EuFe_2As_2^{[HP]}$	$I4/mmm$	3.989	10.006	105.5	117.71	37	50
$SmFFeAs^{[AP]}$	$P4/nmm$	3.939	8.503	110.21	109.10	56	this work

[a]"HP" denotes high pressure, and "AP" denotes ambient pressure.

materials have no magnetic transition at ~12 K.[34,35] Perhaps it could be due to the appearance of the Sm^{2+}-ion-induced magnetic ordered state, in analogy with the preceding studies on Eu^{2+} and Nd^{3+}.[44,45] The superconducting shield fraction is ~19% at 4 K in the ZFC process. The very small volume fraction could be due to the existence of impurities. In many reports, the sample quality judged from XRD is quite good but the superconducting volume fraction is small,[46] which does not affect the confirmation of its superconductivity. In summary, the small superconducting volume fraction should be attributed to the contribution of magnetic impurities (even very small) and the air-sensitivity of sample. The FC curve showed the fraction of 13% at 4 K related to a Meissner volume. The FC measurement shows diamagnetism reduction below T_c, which is caused by the flux pinning.[47] In addition, we find a small and almost disappearing paramagnetic Pauli-like magnetic susceptibility when the temperature is above the T_c value.[47] Herein, a comparison of the transition temperature (T_c) was made among the as-synthesized SmFFeAs and other representative high-T_c compounds. As presented in Table 2, SmFFeAs shows a much higher T_c under ambient pressure without requiring either explicit doping or pressure. In particular, the T_c value of ~56 K has exceeded the transition temperature record (~30 K) reported for the 1111-type superconductors without extrinsic doping.[32]

Figure 5 presents the temperature dependence of resistivity for the as-synthesized and annealed pellet SmFFeAs samples, respectively. It is recognizable that both samples exhibit metallic behavior between the transition temperature and 200 K, a quasi-linear relationship between resistivity and temperature without anomaly investigated as an antiferromagnetic SDW in an undoped 1111-type compound. As represented in previous work,[1,3−6] superconductivity is mostly attained when extrinsic doping or defects are introduced to suppress SDW or cause phase transitions. And it reflects the competitive relationship between the antiferr-omagnetic SDW and superconductivity. Consequently, the absence of antiferromagnetic SDW provides the possibility of superconductivity in our parent compound. For the as-synthesized sample, the $\rho(T)$ curve can be well-fitted using the formula $\rho(T) = \rho_0 + AT^{\alpha}$ between 70 K and 100 K (the red dashed line in Figure 5a), indicating a Fermi liquid behavior of the compound, with $\rho_0 = 2.23 \times 10^{-3}$ Ω cm, $A = 1.53 \times 10^{-7}$ Ω cm K^{-2}, and $\alpha = 2.00$. The T_c^{onset} value is equal to 56 K and the zero-resistance critical temperature (T_c^0) is observed at ~10 K. As shown in the inset of Figure 5a, as the magnetic field increased from 0 to 2 T, the change of the T_c^{onset} is negligible. Similar behavior was also observed in other superconductors.[47] The anomaly between 20 K and 40 K may be due to some magnetic impurities. And, in the magnetic field of 8 T, we found that the

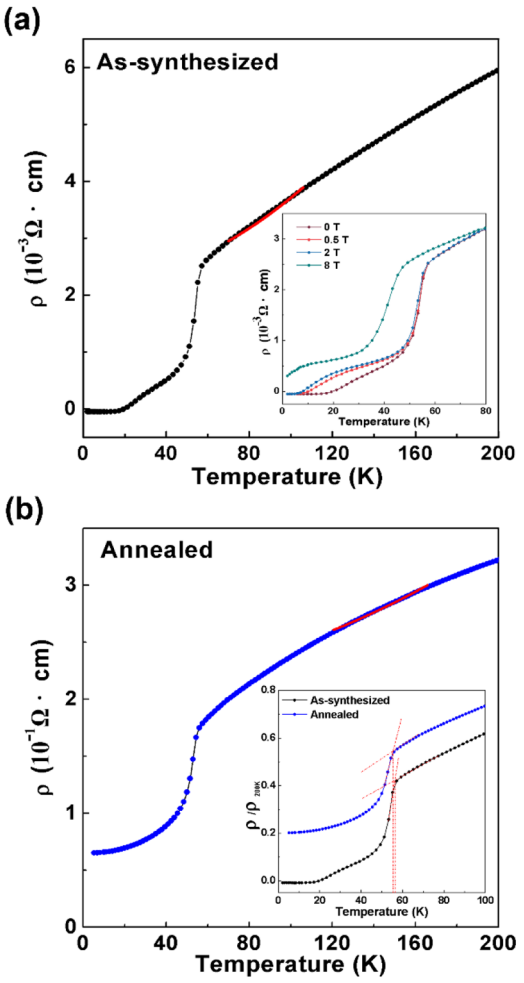

Figure 5. Temperature dependence of resistivity $\rho(T)$ of the (a) as-synthesized sample and (b) annealed sample at zero field. The inset in panel (a) shows the resistivity as a function of T of the as-synthesized sample under zero magnetic field and under 0.5, 2, and 8 T. The inset in panel (b) shows the enlarged ratio curves of $\rho/\rho_{200\,K}$, as a function of T of the as-synthesized and annealed samples near T_c, respectively.

T_c^{onset} moved to lower temperature and the zero resistance was absent.

As shown in Figure 5b, between 120 and 165 K, the $\rho(T)$ curve also shows a T^2 dependence in its normal-state electrical resistivity (the red dashed line in Figure 5b) with $\rho_0 = 2.16 \times 10^{-1}$ Ω cm and $A = 3.02 \times 10^{-6}$ Ω cm K^{-2}. Compared with the as-synthesized sample, the T_c^{onset} slightly moves to lower temperature (see the inset in Figure 5b). In addition, note that, although the measurement results show signs of superconducting transition, the resistivity does not go to zero.

DOI: 10.1021/acs.inorgchem.9b02464
Inorg. Chem. XXXX, XXX, XXX−XXX

The evident change in resistivity between as-synthesized and annealing samples is likely attributed to the change of crystal quality as the effect of annealing treatment.[47] According to the detailed results shown in Figure S2 in the Supporting Information, it can be seen that the diffraction peaks are slightly sharper in the as-synthesized sample than in the annealed one. Moreover, more impurities were observed after annealing, which could be due to the partial decomposition. The decrease in crystallinity results in an overall increase in resistivity.

Here, we discuss the origin of superconductivity in the SmFFeAs sample. Some may argue whether the occurrence of superconductivity in the SmFFeAs seems to be attributed to the electron doping, because the lattice parameters are similar to the F-doped SmOFeAs phase, which may happen if the oxygen leaked into the samples. However, we can rule out this possibility by following arguments. First, all the precursors were stored in the glovebox. All the weighting and mixing processes were performed in the glovebox where the amount of oxygen is limited under a low level (<1 ppm). The reactions then were performed with all the precursors being sealed into the quartz tube. There is no chance for oxygen going into the samples. And the precursors as well as the final product are monophasic without oxygen-containing phases from the XRD measurements (shown in Figures S3 and S4 in the Supporting Information). Second, the XPS results (shown in Figure 3e) suggest that no traces of O-doped samples could be detected, as mentioned above.

We speculate that one possibility for explaining the superconductivity in this system could be due to the $FeAs_4$ tetrahedron tending toward regular tetrahedron without distortion. Prior research[51] presented an idea that T_c increases when the $FeAs_4$ tetrahedron is transformed toward an ideal tetrahedron with the As−Fe−As bond angle tending toward 109.47°. To confirm the relationship between the As−Fe−As bond angles and superconductivity, we show the values with the As−Fe−As bond angles of SmFFeAs and other undoped iron-based compounds in Figure 6 (data are taken from the literature[1,11,12,21−27,30−32,44,46,52]). It turned out that the angles of the compounds exhibiting higher T_c values are mostly distributed around 109.47° (see Figures S5 and S6 in the Supporting Information). However, considering the performances of some compounds (ThNFeAs, LaOFeP, KFe_2As_2, etc.), the angles of the tetrahedron further deviating from the ideal angle seems to be more favorable to the introduction of superconductivity. Hence, this type of correlation between crystal structure and superconductivity could not account for all the iron-based superconductors. While taking both the two As(P)−Fe-As(P) angles into account synthetically (see Figure 6), we could clearly generalize a relationship between superconductivity and crystal structure. It could be observed that almost all of the nonsuperconducting iron-based parent compounds, the undoped 1111-type iron-based superconductors and the self-doped SmFFeAs fall on this line (the red dashed line in Figure 6), which can be fitted by the formula $\beta = 160.87-0.469 \times \alpha$. Perhaps in the future work, we could roughly classify a compound as a nonsuperconducting parent compound, undoped, or self-doped 1111-type iron-based superconductor by whether its structural parameters satisfy the above-summarized formula.

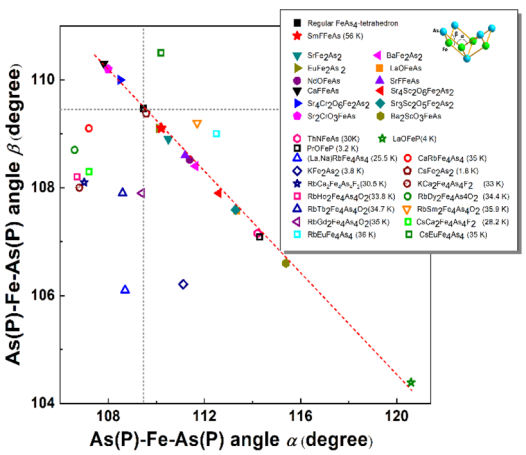

Figure 6. As(P)−Fe−As(P) bond angles of SmFFeAs and other iron arsenide-based parent compounds. The definitions of the As−Fe−As bond angles α and β are illustrated on the right side with a $FeAs_4$ tetrahedron. Angle α represents the intraplanar bond angle that spans over the As−Fe−As bond in the original plane. Angle β represents the interplanar bond angle that crosses over the bond from one As plane through an Fe atom to another As plane.

Besides, we also note another commonly used parameter for the crystal-structure relationship with superconductivity: the As height from the Fe plane (h_{As}). In some previous works,[53] it has been concluded that the maximum T_c value would be expected by approaching an As height of 1.38 Å. We could see that the h_{As} parameter for the present sample (Table 1, h_{As} = 1.374 Å) is appropriate for producing superconductivity. However, in contrast, the T_c value has a tendency to increase when h_{As} further deviates from the ideal value in many other FeAs-based superconductor systems.[54] Therefore, the As height dependence still calls for further theoretical investigations.

It is known that most FeSCs are realized upon extrinsic chemical doping in parent compounds. Here, we consider that the doping by the material itself may tightly account for the superconductivity in SmFFeAs. As displayed in Figure 3a, the coexistence of Sm^{2+} and Sm^{3+} was revealed in the as-synthesized sample. The mixed valence induces charge transfer, which enables internal electron doping into the conduction bands, leading a positive contribution to the superconductivity. A similar phenomenon of valence mixing was also observed in Eu-containing superconductors.[50,55] The occurrence of superconductivity in many self-doped Eu-containing systems is explained by the fact that the valence mixing makes Eu ions-containing layers allow additional charges to the conduction bands. The conduction bands were self-doped with the transferred electrons. Here, note that the 122-type self-doped superconductor $EuFe_2As_2$ slightly differs from the SmFFeAs in that the valence transition from Eu^{2+} state to Eu^{3+} state only occurs at the pressure range from 3 GPa to 9 GPa.[50] And the As−Fe−As bond angle values for $EuFe_2As_2$ at high pressure deviate far from the regular angle value of 109.47° (as shown in Table 2). However, in our sample, the mixed valence of Sm ions was revealed at ambient pressure. On the other hand, comparing with the case of EuFFeAs,[45] both SmFFeAs and EuFFeAs are the members of 1111-type fluoride-arsenide AeFeAsF materials. However, interestingly, it was found that the anomaly at 153 K for EuFFeAs was observed in the resistivity and magnetic susceptibility without exhibiting superconductivity. Wen et al. proved that one must enable high-level electrons doping in the EuFFeAs system in order to

DOI: 10.1021/acs.inorgchem.9b02464
Inorg. Chem. XXXX, XXX, XXX−XXX

induce superconductivity, based on its positive Hall coefficient (R_H) data.[45] The origin and method to generate mixed valence states of ions (Eu, Sm etc.) still deserve further studies. In the view of many other systems, it is worthy noting that similar self-doping behaviors at ambient pressure have also been found, leading to high-temperature superconductivity, such as $Ba_2Ti_2Fe_2As_4O$[29], $AeAFe_4As_4$ (Ae = Ca, Sr, Eu; A = K, Rb, Cs),[23−25] $ACa_2Fe_4As_4F_2$ (A = K, Rb, Cs),[26,27] etc. Hence, we can see that the self-doping is of potential interest to be a strategy to future explore superconductors.

CONCLUSIONS

We have successfully synthesized an oxygen-free superconductor SmFFeAs with the tetragonal ZrCuSiAs-type structure by utilizing a soft method SSM. Temperature dependence of magnetic susceptibility and electric resistivity demonstrate that the SmFFeAs exhibits a superconducting transition temperature T_c of ∼56 K without requiring either extrinsic doping or pressure. The possible reason for the occurrence of superconductivity is that the existence of mixed valence of Sm ions donated self-doping to SmFFeAs. Nevertheless, further investigation is required in theory and experiment to verify that could be different from other 1111 systems. The discovery of SmFFeAs appends a new member of oxygen-free high-T_c superconductors and we hope that the SmFFeAs can be utilized as a platform to study the mechanism of high-T_c superconductivity.

ASSOCIATED CONTENT

Supporting Information

The Supporting Information is available free of charge on the ACS Publications website at DOI: 10.1021/acs.inorgchem.9b02464.

XPS spectra for the O 1s of the as-obtained sample SmFFeAs; powder X-ray diffraction (XRD) patterns of the as-synthesized and annealed SmFFeAs samples; powder XRD patterns of the precursor LiFeAs and SmFCl; the relationship between the As−Fe−As bond angles and the T_c values of the SmFFeAs and other iron arsenide-based compounds (PDF)

Accession Codes

CSD 1938585 contains the supplementary crystallographic data for this paper. These data can be obtained free of charge via www.ccdc.cam.ac.uk/data_request/cif, or by emailing data_request@ccdc.cam.ac.uk, or by contacting The Cambridge Crystallographic Data Centre, 12 Union Road, Cambridge CB2 1EZ, UK; fax: + 44 1223 336033.

AUTHOR INFORMATION

Corresponding Author

*E-mail: kbtang@ustc.edu.cn.

ORCID

Dan Lin: 0000-0002-0883-9084

Haoliang Huang: 0000-0002-5686-5519

Kaibin Tang: 0000-0002-0398-1196

Author Contributions

The manuscript was written through contributions of all authors. All authors have given approval to the final version of the manuscript.

Notes

The authors declare no competing financial interest.

ACKNOWLEDGMENTS

This work was supported by the National Natural Science Foundation of China (Grant No. 21671182). We would like to thank X. G. Liu for technical assistance.

REFERENCES

(1) Kamihara, Y.; Watanabe, T.; Hirano, M.; Hosono, H. Iron-based layered superconductor La[$O_{1-x}F_x$]FeAs (x = 0.05−0.12) with T_c = 26 K. *J. Am. Chem. Soc.* **2008**, *130* (11), 3296−3297.

(2) McMillan, W. L. Transition Temperature Of Strong-Coupled Superconductors. *Phys. Rev.* **1968**, *167* (2), 331−343.

(3) Chen, X. H.; Wu, T.; Wu, G.; Liu, R. H.; Chen, H.; Fang, D. F. Superconductivity at 43 K in $SmFeAsO_{1-x}F_x$. *Nature* **2008**, *453*, 761−762.

(4) Ren, Z. A.; Yang, J.; Lu, W.; Yi, W.; Che, G. C.; Dong, X. L.; Sun, L. L.; Zhao, Z. X. Superconductivity at 52 K in iron based F doped layered quaternary compound Pr[$O_{1-x}F_x$]FeAs. *Mater. Res. Innovations* **2008**, *12* (3), 105−106.

(5) Zhi-An, R.; Wei, L.; Jie, Y.; Wei, Y.; Xiao-Li, S.; Zheng-Cai; Guang-Can, C.; Xiao-Li, D.; Li-Ling, S.; Fang, Z.; Zhong-Xian, Z. Superconductivity at 55 K in Iron-Based F-Doped Layered Quaternary Compound Sm[$O_{1-x}F_x$]FeAs. *Chin. Phys. Lett.* **2008**, *25* (6), 2215−2216.

(6) Ren, Z.; Yang, J.; Lu, W.; Yi, W.; Shen, X.; Li, Z.; Che, G.; Dong, X.; Sun, L.; Zhou, F.; Zhao, Z.-X. Superconductivity in the iron-based F-doped layered quaternary compound Nd[$O_{1-x}F_x$]FeAs. *Europhys. Lett.* **2008**, *82* (5), 57002.

(7) Yang, J.; Li, Z.-C.; Lu, W.; Yi, W.; Shen, X.-L.; Ren, Z.-A.; Che, G.-C.; Dong, X.-L.; Sun, L.-L.; Zhou, F. Superconductivity at 53.5 K in $GdFeAsO_{1-\delta}$. *Supercond. Sci. Technol.* **2008**, *21* (8), 082001.

(8) Yang, J.; Shen, X. L.; Lu, W.; Yi, W.; Li, Z. C.; Ren, Z. A.; Che, G. C.; Dong, X. L.; Sun, L. L.; Zhou, F.; Zhao, Z. X. Superconductivity in some heavy rare-earth iron arsenide $REFeAsO_{1-\delta}$ (RE = Ho, Y, Dy and Tb) compounds. *New J. Phys.* **2009**, *11* (2), 025005.

(9) de la Cruz, C.; Huang, Q.; Lynn, J. W.; Li, J.; Ratcliff, W., II; Zarestky, J. L.; Mook, H. A.; Chen, G. F.; Luo, J. L.; Wang, N. L.; Dai, P. Magnetic order close to superconductivity in the iron-based layered $LaO_{1-x}F_xFeAs$ systems. *Nature* **2008**, *453* (7197), 899−902.

(10) Wolff, K. K.; Shlyk, L.; Bischoff, M.; Rose, E.; Niewa, R.; Schleid, T. Synthesis and Characterization of Superconducting $Ca_{1-x}Na_xFFeAs$. *Materials* **2014**, *7* (3), 1984−1994.

(11) Han, F.; Zhu, X.; Mu, G.; Cheng, P.; Wen, H. H. SrFeAsF as a parent compound for iron pnictide superconductors. *Phys. Rev. B: Condens. Matter Mater. Phys.* **2008**, *78* (18), 180503.

(12) Matsuishi, S.; Inoue, Y.; Nomura, T.; Yanagi, H.; Hirano, M.; Hosono, H. Superconductivity induced by co-doping in quaternary fluoroarsenide CaFeAsF. *J. Am. Chem. Soc.* **2008**, *130* (44), 14428−14429.

(13) Wu, G; Xie, Y L; Chen, H; Zhong, M; Liu, R H; Shi, B C; Li, Q J; Wang, X F; Wu, T; Yan, Y J; Ying, J J; Chen, X H Superconductivity at 56 K in samarium-doped SrFeAsF. *J. Phys.: Condens. Matter* **2009**, *21* (21), 1118−1129.

(14) Chong, S. V.; Hashimoto, S.; Yamaguchi, H.; Kadowaki, K. Neodymium-Doping Induced Superconductivity in 1111-SrFeAsF Iron-Pnictide System. *J. Supercond. Novel Magn.* **2010**, *23* (8), 1479−1484.

(15) Shlyk, L.; Bischoff, M.; Rose, E.; Niewa, R. Superconductivity at T_c = 36.5 K in Na-Substituted $SrFe_2As_2$ Single Crystals. *Adv. Sci. Technol.* **2014**, *95*, 150−155.

(16) Sun, G. L.; Sun, D. L.; Konuma, M.; Popovich, P.; Boris, A.; Peng, J. B.; Choi, K. Y.; Lemmens, P.; Lin, C. T. Single Crystal Growth and Effect of Doping on Structural, Transport and Magnetic Properties of $A_{1-x}K_xFe_2As_2$ (A = Ba, Sr). *J. Supercond. Novel Magn.* **2011**, *24* (5), 1773−1785.

(17) Zhao, K.; Liu, Q. Q.; Wang, X. C.; Deng, Z.; Lv, Y. X.; Zhu, J. L.; Li, F. Y.; Jin, C. Q. Superconductivity above 33 K in $(Ca_{1-x}Na_x)Fe_2As_2$. *J. Phys.: Condens. Matter* **2010**, *22* (22), 1842.

DOI: 10.1021/acs.inorgchem.9b02464
Inorg. Chem. XXXX, XXX, XXX−XXX

(18) Zhiyong, L.; Hongli, S.; Lin, M.; Junjing, Z.; Baorong, N.; Zhichao, G.; Binjie, Y.; Min, L.; Ziping, W.; Meiling, Z. Effect of F Doping on Fabrication and Superconductivity of $SmO_{1-x}F_{\delta}FeAs$ Compound. *Rare Metal Mater. Eng.* **2012**, *41* (7), 1144−1148.
(19) Kihou, K.; Saito, T.; Ishida, S.; Nakajima, M.; Tomioka, Y.; Fukazawa, H.; Kohori, Y.; Ito, T.; Uchida, S.-i.; Iyo, A.; Lee, C.-H.; Eisaki, H. Single Crystal Growth and Characterization of the Iron-Based Superconductor KFe_2As_2 Synthesized by KAs Flux Method. *J. Phys. Soc. Jpn.* **2010**, *79*, 124713.
(20) Bukowski, Z.; Weyeneth, S.; Puzniak, R.; Karpinski, J.; Batlogg, B. Bulk superconductivity at 2.6 K in undoped $RbFe_2As_2$. *Phys. C* **2010**, *470*, S328−S329.
(21) Tafti, F. F.; Ouellet, A.; Juneau-Fecteau, A.; Faucher, S.; Lapointe-Major, M.; Doiron-Leyraud, N.; Wang, A. F.; Luo, X. G.; Chen, X. H.; Taillefer, L. Universal V-shaped temperature-pressure phase diagram in the iron-based superconductors KFe_2As_2, $RbFe_2As_2$, and $CsFe_2As_2$. *Phys. Rev. B: Condens. Matter Mater. Phys.* **2015**, *91* (5), 054511.
(22) Gooch, M.; Lv, B.; Sasmal, K.; Tapp, J. H.; Tang, Z. J.; Guloy, A. M.; Lorenz, B.; Chu, C. W. Superconductivity in ternary iron pnictides: AFe_2As_2 (A = alkali metal) and LiFeAs. *Phys. C* **2010**, *470* (22), S276−S279.
(23) Liu, Y.; Liu, Y. B.; Chen, Q.; Tang, Z. T.; Jiao, W. H.; Tao, Q.; Xu, Z. A.; Cao, G. H. A New Ferromagnetic Superconductor: $CsEuFe_4As_4$. *Sci. Bull.* **2016**, *61* (15), 1213−1220.
(24) Iyo, A.; Kawashima, K.; Kinjo, T.; Nishio, T.; Ishida, S.; Fujihisa, H.; Gotoh, Y.; Kihou, K.; Eisaki, H.; Yoshida, Y. New-Structure-Type Fe-Based Superconductors: $CaAFe_4As_4$ (A = K, Rb, Cs) and SrAFe4As4 (A = Rb, Cs). *J. Am. Chem. Soc.* **2016**, *138* (10), 3410−3415.
(25) Liu, Y.; Liu, Y.-B.; Tang, Z.-T.; Jiang, H.; Wang, Z.-C.; Ablimit, A.; Jiao, W.-H.; Tao, Q.; Feng, C.-M.; Xu, Z.-A.; Cao, G.-H. Superconductivity and Ferromagnetism in Hole-Doped $RbEuFe_4As_4$. *Phys. Rev. B: Condens. Matter Mater. Phys.* **2016**, *93* (21), 214503.
(26) Wang, Z.-C.; He, C.-Y.; Wu, S.-Q.; Tang, Z.-T.; Liu, Y.; Cao, G.-H. Synthesis, crystal structure and superconductivity in $RbLn_2Fe_4As_4O_2$ (Ln = Sm, Tb, Dy and Ho). *Chem. Mater.* **2017**, *29* (4), 1805−1812.
(27) Wang, Z. C.; He, C. Y.; Wu, S. Q.; Tang, Z. T.; Liu, Y.; Ablimit, A.; Feng, C. M.; Cao, G. H. Superconductivity in KCa2Fe4As4F2 with Separate Double Fe2As2 Layers. *J. Am. Chem. Soc.* **2016**, *138* (25), 7856−7859.
(28) Zhu, X.; Han, F.; Mu, G.; Cheng, P.; Shen, B.; Zeng, B.; Wen, H. H. Transition of stoichiometric Sr_2VO_3FeAs to a superconducting state at 37.2 K. *Phys. Rev. B: Condens. Matter Mater. Phys.* **2009**, *79* (22), 1377−1381.
(29) Sun, Y.-L.; Jiang, H.; Zhai, H.-F.; Bao, J.-K.; Jiao, W.-H.; Tao, Q.; Shen, C.-Y.; Zeng, Y.-W.; Xu, Z.-A.; Cao, G.-H. $Ba_2Ti_2Fe_2As_4O$: A new superconductor containing Fe_2As_2 layers and Ti_2O sheets. *J. Am. Chem. Soc.* **2012**, *134* (31), 12893−12896.
(30) Kamihara, Y.; Hiramatsu, H.; Hirano, M.; Kawamura, R.; Yanagi, H.; Kamiya, T.; Hosono, H. Iron-based layered superconductor: LaOFeP. *J. Am. Chem. Soc.* **2006**, *128* (31), 10012−10013.
(31) Baumbach, R. E.; Hamlin, J. J.; Shu, L.; Zocco, D. A.; Crisosto, N. M.; Maple, M. B. Superconductivity in LnFePO (Ln = La, Pr and Nd) single crystals. *New J. Phys.* **2009**, *11* (2), 025018.
(32) Wang, C.; Wang, Z. C.; Mei, Y. X.; Li, Y. K.; Li, L.; Tang, Z. T.; Liu, Y.; Zhang, P.; Zhai, H. F.; Xu, Z. A.; Cao, G.-H. A New ZrCuSiAs-Type Superconductor: ThFeAsN. *J. Am. Chem. Soc.* **2016**, *138* (7), 2170−2173.
(33) Frankovsky, R.; Marchuk, A.; Pobel, R.; Johrendt, D. Synthesis of $LaO_{1-x}F_xFeAs$ (x = 0−0.15) via solid state metathesis reaction. *Solid State Commun.* **2012**, *152* (8), 632−634.
(34) Katsuraki, H.; Achiwa, N. The Magnetic Structure of Fe_2As. *J. Phys. Soc. Jpn.* **1966**, *21* (11), 2238−2243.
(35) Segawa, K.; Ando, Y. Magnetic and Transport Properties of FeAs Single Crystals. *J. Phys. Soc. Jpn.* **2009**, *78* (10), 104720.
(36) Hernan, L.; Morales, J.; Sanchez, L.; Santos, J.; Rodriguez-Castellon, E.; Martinez, J. L. X-ray Diffraction, XPS, and Magnetic Properties of Lanthanide-Based Misfit-Layered Sulfides Intercalated with Cobaltocene. *Chem. Mater.* **2000**, *12*, 3792−3797.
(37) Brown, I. D.; Altermatt, D. Bond-Valence Parameters Obtained from a Systematic Analysis of the Inorganic Crystal Structure Database. *Acta Crystallogr., Sect. B: Struct. Sci.* **1985**, *B41*, 244−247.
(38) Biesinger, M. C.; Payne, B. P.; Grosvenor, A. P.; Lau, L. W. M.; Gerson, A. R.; Smart, R. S. C. Resolving surface chemical states in XPS analysis of first row transition metals, oxides and hydroxides: Cr, Mn, Fe, Co and Ni. *Appl. Surf. Sci.* **2011**, *257* (7), 2717−2730.
(39) Dedryvère, R.; Maccario, M.; Croguennec, L.; Le Cras, F.; Delmas, C.; Gonbeau, D. X-Ray Photoelectron Spectroscopy Investigations of Carbon-Coated Li_xFePO_4 Materials. *Chem. Mater.* **2008**, *20* (22), 7164−7170.
(40) Shuttleworth, D. Preparation of metal-polymer dispersions by plasma techniques. An ESCA investigation. *J. Phys. Chem.* **1980**, *84* (12), 1629−1634.
(41) Flinn, B. J.; Mcintyre, N. S. Studies of the UV/Ozone oxidation of GaAs using angle-resolved x-ray photoelectron spectroscopy. *Surf. Interface Anal.* **1990**, *15* (1), 19−26.
(42) Liang, H.; Hong, Y.; Zhu, C.; Li, S.; Chen, Y.; Liu, Z.; Ye, D. Influence of partial Mn-substitution on surface oxygen species of $LaCoO_3$ catalysts. *Catal. Today* **2013**, *201*, 98−102.
(43) Zhang, Y.; Chen, Y. L.; Cui, Y. J.; Cheng, C. H.; Zhang, H.; Zhao, Y. A study of the Fe-based superconductor$SmFeAsO_{1-x}F_x$ by x-ray photoelectron spectroscopy. *Supercond. Sci. Technol.* **2009**, *22* (1), 015007.
(44) Kawashima, K.; Kinjo, T.; Nishio, T.; Ishida, S.; Fujihisa, H.; Gotoh, Y.; Kihou, K.; Eisaki, H.; Yoshida, Y.; Iyo, A. Superconductivity in Fe-Based Compound $EuAFe_4As_4$(A = Rb and Cs). *J. Phys. Soc. Jpn.* **2016**, *85* (6), 064710.
(45) Zhu, X.; Han, F.; Cheng, P.; Mu, G.; Shen, B.; Zeng, B.; Wen, H. H. Parent phase and superconductors in the fluorine derivative family. *Phys. C* **2009**, *469* (9), 381−384.
(46) Ying, T. P.; Chen, X. L.; Wang, G.; Jin, S. F.; Zhou, T. T.; Lai, X. F.; Zhang, H.; Wang, W. Y. Observation of superconductivity at 30 ∼ 46 K in $AxFe_2Se_2$ (A = Li, Na, Ba, Sr, Ca, Yb, and Eu). *Sci. Rep.* **2012**, *2*, 426.
(47) Xu, H. S.; Wang, X. X.; Gao, Z.; Huang, H. L.; Long, Y. Z.; Lu, Y. L.; Tang, K. B. New alkali-metal and 1,2-Diaminopropane intercalated superconductor $Li_x(C_3H_{10}N_2)_yFe_2Se_2$ with T_c = 45 K. *J. Alloys Compd.* **2018**, *735*, 2053−2057.
(48) Wang, C.; Li, L.; Chi, S.; Zhu, Z.; Ren, Z.; Li, Y.; Wang, Y.; Lin, X.; Luo, Y.; Jiang, S.; Xu, X.; Cao, G.; Xu, Z. Thorium-doping-induced superconductivity up to 56 K in $Gd_{1-x}Th_xFeAsO$. *Europhys. Lett.* **2008**, *83* (6), 67006.
(49) Shahi, P.; Sun, J. P.; Wang, S. H.; Jiao, Y. Y.; Chen, K. Y.; Sun, S. S.; Lei, H. C.; Uwatoko, Y.; Wang, B. S.; Cheng, J. G. High-T_c superconductivity up to 55 K under high pressure in a heavily electron doped $Li_{0.36}(NH_3)_yFe_2Se_2$ single crystal. *Phys. Rev. B: Condens. Matter Mater. Phys.* **2018**, *97* (2), 020508.
(50) Uhoya, W.; Tsoi, G.; Vohra, Y. K.; Mcguire, M. A.; Sefat, A. S.; Sales, B. C.; Mandrus, D.; Weir, S. T. Anomalous compressibility effects and superconductivity of $EuFe_2As_2$ under high pressures. *J. Phys.: Condens. Matter* **2010**, *22* (29), 292202.
(51) Lee, C.-H.; Iyo, A.; Eisaki, H.; Kito, H.; Teresa Fernandez-Diaz, M.; Ito, T.; Kihou, K.; Matsuhata, H.; Braden, M.; Yamada, K. Effect of Structural Parameters on Superconductivity in Fluorine-Free $LnFeAsO_{1-y}$ (Ln = La, Nd). *J. Phys. Soc. Jpn.* **2008**, *77* (8), 083704.
(52) Ogino, H.; Katsura, Y.; Horii, S.; Kishio, K.; Shimoyama, J.-i. New iron-based arsenide oxides $(Fe_2As_2)(Sr_4M_2O_6)$ (M = Sc, Cr). *Supercond. Sci. Technol.* **2009**, *22* (8), 085001.
(53) Mizuguchi, Y.; Hara, Y.; Deguchi, K.; Tsuda, S.; Yamaguchi, T.; Takeda, K.; Kotegawa, H.; Tou, H.; Takano, Y. Anion height dependence of T_c for the Fe-based superconductor. *Supercond. Sci. Technol.* **2010**, *23*, 054013.
(54) Wang, Z.; He, C.; Tang, Z.; Wu, S.; Cao, G. Crystal structure and superconductivity at about 30 K in $ACa_2Fe_4As_4F_2$ (A = Rb, Cs). *Sci. China Mater.* **2017**, *60* (1), 83−89.

DOI: 10.1021/acs.inorgchem.9b02464
Inorg. Chem. XXXX, XXX, XXX−XXX

(55) Zhai, H.-F.; Zhang, P.; Wu, S.-Q.; He, C.-Y.; Tang, Z.-T.; Jiang, H.; Sun, Y.-L.; Bao, J.-K.; Nowik, I.; Felner, I.; Zeng, Y.-W.; Li, Y.-K.; Xu, X.-F.; Tao, Q.; Xu, Z.-A.; Cao, G.-H. Anomalous Eu valence state and superconductivity in undoped $Eu_3Bi_2S_4F_4$. *J. Am. Chem. Soc.* **2014**, *136* (43), 15386−15393.

DOI: 10.1021/acs.inorgchem.9b02464
Inorg. Chem. XXXX, XXX, XXX−XXX